www.ijbar.org
ISSN 2249-3352 (P) 2278-0505 (E)
Cosmos Impact Factor-5.86

Power management and control of EV charger with V2G and G2V abilities of EV fed with Grid tied PV system

Banothu Saritha, K.Prakash chary
1, PG Scholar, Department of Electrical and Electronics Engineering
2, Assistant Professor, Department of Electrical and Electronics Engineering
Vaagdevi College Of Engineering, Bollikunta, Warangal(Dt), TS, India.
bbsaritha12@gmail.com

Abstract: Here, we introduce a PV-based off-board charging system that is grid-integrated via a VSC. The grid-connected charger is controlled by the JLHCAF algorithm, which efficiently monitors the load current's basic component, provides a quick dynamic reaction, and is resistant to impulsive interference. Competing sparsity-aware robust algorithms are surpassed by this algorithm. Incorporating a proportional-resonant (PR) controller for error correction significantly improved the system's performance. By removing steady-state faults, the PR controller greatly enhances the system's capability to manage sinusoidal AC signals, especially in grid-connected situations. The PR controller improves stability under dynamic loading situations and achieves zero steady-state error compared to the standard proportional-integral (PI) controller. It also leads to superior harmonic compensation. For electric vehicle (EV) charging and discharging, the bidirectional buck-boost converter is controlled by the cascaded PR controller. The converter operates in buck mode when charging and boost mode when discharging. Adaptive maximum power point tracking (MPPT) is used to derive the reference DC link voltage in order to maximise power extraction from the PV source. Due to its bidirectional capabilities, the system can sustain important nonlinear loads and perform many tasks, including grid-to-vehicle (G2V), vehicle-to-grid (V2G), PV source-to-grid (PV2G), vehicle-to-home (V2H), and PV source-to-vehicle (PV2V). By utilising the PR controller, the control method not only reduces total harmonic distortion (THD) more effectively than PI-controlled systems, but it also guarantees compliance with IEEE power quality requirements. Simulations and experimental prototypes were used to test the system's performance under dynamic settings, which included changes in PV insolation and fluctuations in home load. The results showed that the system effectively decreased THD and improved harmonic suppression.

Key Words: PV system, MPPT, VSC, proportional-resonant controller, proportional-integral controller, Electric vehicle, vehicle to grid and grid to vehicle.

I. Introduction

Electric vehicles (EVs) are quickly becoming the preferred mode of transportation as people become more conscious of the environmental impacts of fossil fuels and their finite supply. Compared to traditional cars, electric vehicles have a number of benefits, such as a lack of pollution, excellent mechanical stability, and the capacity to utilise electricity as fuel, which may be produced in a variety of ways [1]. A charging infrastructure must be developed if the percentage of electric vehicles in the transportation industry is to rise. While both on-board and off-board chargers are available, the benefits of on-board chargers (OBCs) include a simple BMS and a low price tag [2]. However, rapid charging is possible using off-board chargers.

Nevertheless, power quality (PQ) concerns might arise while charging EVs through the grid. This is because EV loads often include power electronic devices, which causes voltage drops and a great deal of noise during charging and preconditioning [3]. One reliable approach that stands out is P&O control, which has low learning curves, fast convergence rates, and is easy to apply [6-8]. A simplified power regulation method for maximum power point tracking (MPPT) in grid-connected photovoltaic systems is described in reference [9]. Furthermore, a new kind of electric car charging station, controlled by a Type-1 vehicle connector and helped by solar energy at level-2, is proposed and executed in Reference [10]. To keep an eye on power quality when PV isn't working, the DSTATCOM mode is used [11–13]. Control methods used for this include synchronous reference frame (SRF) and least mean square (LMS). Having said that, the SRF control technique isn't very good and has a big steady-state inaccuracy. The adaptive control algorithm, on the other hand, responds quickly and has a lower steady-state error when subjected to a nonlinear grid load. Ref. [14] makes extensive use of adaptive control, which automatically modifies the controller parameters to account for the nonlinear load. Particularly noteworthy is the JLHCAF adaptive control approach, which exhibits both rapid convergence and strong dynamic performance.

To enable battery charging and regulate the DC link voltage, a DC-DC stage is required [15]. When demand is low, electric vehicles can draw power from the grid, and when demand is high, they can do the opposite. The grid-to-vehicle (G2V) mode involves charging the battery using grid power, while the vehicle-to-grid (V2G) mode is used for charging the battery using vehicle power [16-17]. The Luo power factor pre-regulator (PFP) [18] could be the key to an affordable, high-power, and high-quality electric vehicle (EV) battery charger. The current travelling between the two sandwiched Luo converter cells is cut. In reference [19], a three-level quadratic converter is used to accomplish high voltage gain and improve the on-board characteristics of electric vehicle battery chargers. Among these features are the following: compatibility with a broad range of input voltages (85-265 V), smaller filter, improved efficiency, faster dynamic characteristics, and lower voltage stress. According to Reference [20], the solar PV array and a BES are the main components used to charge the battery of the electric vehicle. If the storage battery fails or the solar PV array isn't generating enough power, charging stations can automatically draw electricity from the grid or a diesel generator (DG) set to run at a maximum efficiency of 80% to 85%. References [21-22] detail several operational modes for charging stations based on photovoltaic (PV) arrays, batteries, the grid, and diesel generator (DG) sets, all with the goal of providing continuous charging and uninterrupted electricity to residential loads. In order to optimise the charging profile for electric vehicles (EVs), a multi-objective EV charging installation is presented in Ref. [23] using a sigma-modified adaptive control approach. In spite of several grid imperfections and parametric uncertainties, the current approach offers a rapid control update that leads to well-controlled charging dynamics. This paper lays out its key arguments and provides evidence to back them up. Making a JLHCAF-based VSC adaptive control system. The method's recursive improved signal, high reliability, and good convergence rate all contribute to better power quality [24-27]. (2) Different modes of functioning. Depending on the configuration, the system can act as a PV array to vehicle (PVA2V), a PV array to grid (PVA2G), or a PV array to home (PVS2H) when they are present. Additionally, the messages "vehicle to grid" (V2G) and "grid to vehicle" (G2V) are displayed. By adjusting the variable speed controller (VSC), it can be operated as a grid-to-home (G2H) system when PV generation is down and battery power is low. There are three potential destinations for the power generated by photovoltaics (PV): the home, the utility grid, and the vehicle. G2V and V2G, which stand for vehicle to grid, are also shown. In grid-to-home (G2H) operation, the VSC is used as a compensating unit when the PV power is insufficient and there is insufficient energy from the BES reduced electricity consumption.

II. Proposed System topology

Figure 1 shows the PV array off-board charging system. A diode bridge rectifier and a series RL branch create a nonlinear load in this system, which is fed by a single-phase AC source connected at the PCC. Four integrated gate bipolar transistor (IGBT) switches form the bridge of the voltage source converter (VSC). The DC link capacitor connects the PV source and the buck-boost DC-DC converter through a shared connection node on the DC side of the VSC. By connecting a number of modules in series and parallel, we can create a PV source. Then, we can use the P&O method to determine the PV array's voltage and current. To control the DC link voltage and make charging and discharging the batteries easier, a DC-DC Buck-boost converter is linked to the DC bus capacitor. The control for the DC-DC converter is made up of cascaded PI controllers, with the voltage loop forming the outer loop and the current loop the inner loop. The DC-DC converter allows for the attachment of a rechargeable electric vehicle battery to the system. Tab. 2 shows the charger's specifications.

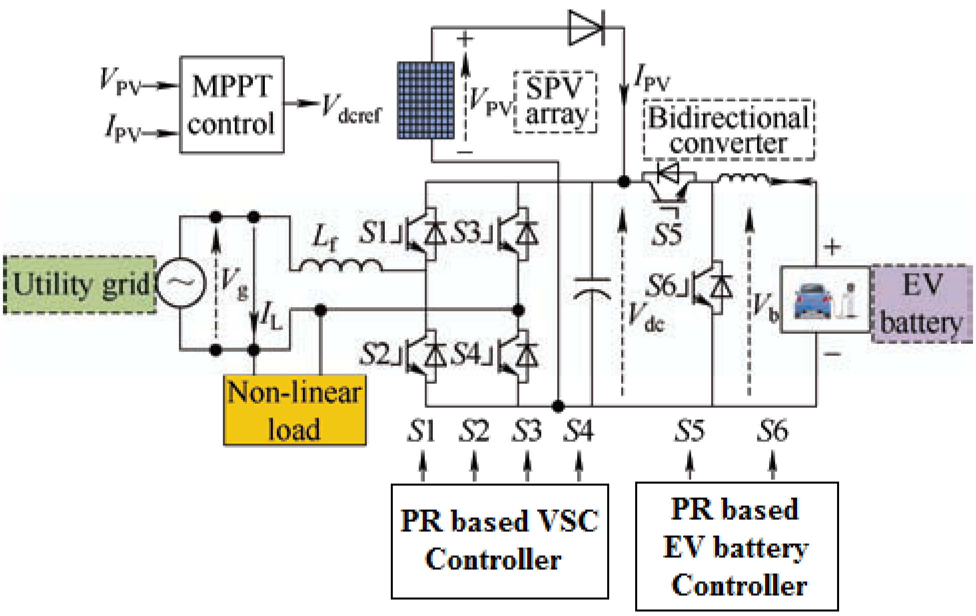

.

Figure 1 Proposed system implementation

a) Control structures

To regulate the current, an adaptive filter called JLHCAF is used. This filter is based on the joint logarithmic hyperbolic cosine. The forward term is also used to stabilise the PV array's volatility. To manage the DC bus voltage and make the two-stage EV charging station work with grid integration, the cascaded control technique uses two PI regulators. A bidirectional converter ensures steady and reliable charging system operation by controlling the DC link voltage. The correct functioning depends on sensing the current flowing through the battery.

Table 4.1 Test System Parameters

Parameter	Value
Battery voltage/V	120
Battery/(A·h)	84
Load resistance R_L/Ω	44.8
Load inductance L_L/mH	97
Bidirectional converter inductance/mH	2.9
Filter parameter L_f, R_f, C_f	5 mH, 5 Ω, 20 μF
Switching frequency/kHz	10
DC link capacitance C_{dc}/μF	2 350

b) JLHCAF based VSC controller

In Fig. 2, we can see the JLHCAF adaptive filter schematic. By predicting the fundamental load current, it improves the charging system's controllability and helps determine the fundamental component of the load current. Reducing the loads' higher-order harmonics allows one to extract the nonlinear load's fundamental signal.

$$V_\alpha = V_g$$

$$V_\beta = V_\alpha - \frac{\pi}{2}$$

$$V_t = \sqrt{V_\alpha^2 + V_\beta^2}$$

$$u_t = \frac{V_g}{V_t}$$

$$z(t+1) = z(t) + \mu \tanh[\lambda e(t)]x(t) - \rho \tanh[\alpha w(t)]$$

$$e(t) = i_L(t) - z(t) \cdot u_t$$

$$I_{FFT} = \frac{2P_{pv}}{V_t}$$

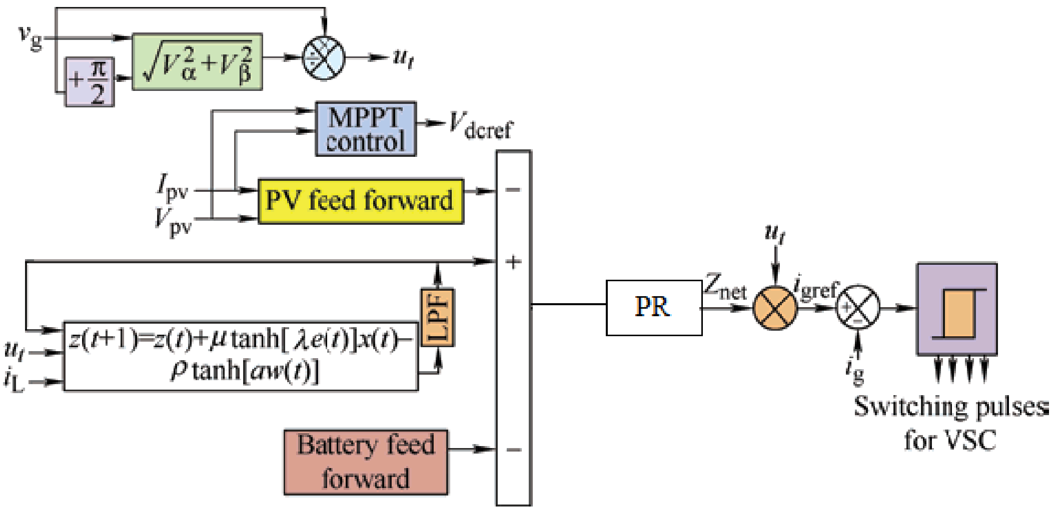

Figure 2 JLHCAF with PR based VSC control

$$z(t)_{net} = z(t) + I_{FFT} + I_{bat}$$

$$i_{gref} = z_{net} \cdot u_t$$

By comparing the igref with ig, the pulses for the hysteresis controller can be generated. In this method, the grid-integrated off-board charging mechanism is controlled by the gate signals created for VSC.

c) Control for DC link voltage

With cascaded PI controllers, you may manage the voltage of the DC link and the current flowing through the battery. Both the external voltage and the internal current are controlled by separate loops in the arrangement, as shown in Figure 3. It is possible to use the voltage PI controller with both the measured and reference DC voltages. After that, it generates the current control loop's reference current by signalling the current or inner PI controller. By comparing the observed current to the summer reference current, we ensure that the PI controller can comprehend the data. A converter's buck or boost mode can be determined by looking at the loss component, which is shown by the PI controller's output.

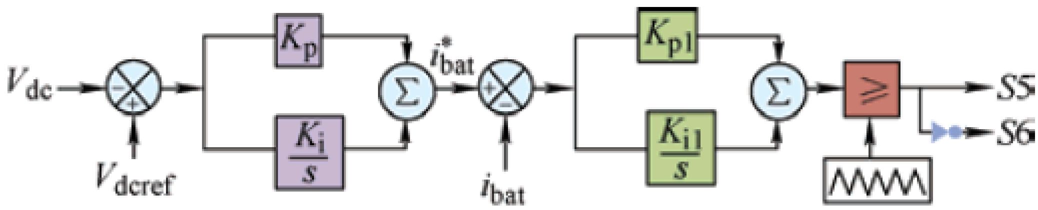

Figure 3 Proposed controller

When using G2V, how does the buck operation function? Subjecting the DC link capacitor to high power loads causes it to undergo a negative loss component. The charging process begins when the converter enters buck mode and begins pouring power into the battery. This configuration enhances the system's power and is compatible with the G2V philosophy. Boost mode of operation/V2G method. The loss component becomes positive as the power level of the DC link capacitor decreases due to factors such as generation loss, grid-side difficulties, or poor solar irradiation. When the battery is dead, it enters boost mode and sends electricity back to the grid using the voltage-to-grid (V2G) technique.

$$(400 - V_{dc}) \times \left(K_p + \frac{K_i}{s} \right) = I^*_{bat}$$

$$D = \left(I^*_{bat} - I_{bat} \right)\left(K_{p1} + \frac{K_{i1}}{s} \right)$$

III. Simulated results

EV charging and discharge operations

Till 0.3 system under floating, G2V from 0.3 s to 0.4 s, and V2G from 0.4 s to 0.5 s modes are shown in Fig. 4. Dynamic system performance from t = 0.25 s to 0.30 s. But due to battery current reversal, the battery charged from t = 0.30 s and 0.40 s. The G2V mode is when the electric vehicle's battery gets juice based on the grid. By increasing the current through the battery and maintaining its voltage at its respective values, the battery is depleted from 0.40 s to 0.50 s. Power is sent from the electric vehicle's battery to the power grid in this mode, which is called V2G mode.

www.ijbar.org
ISSN 2249-3352 (P) 2278-0505 (E)
Cosmos Impact Factor-5.86

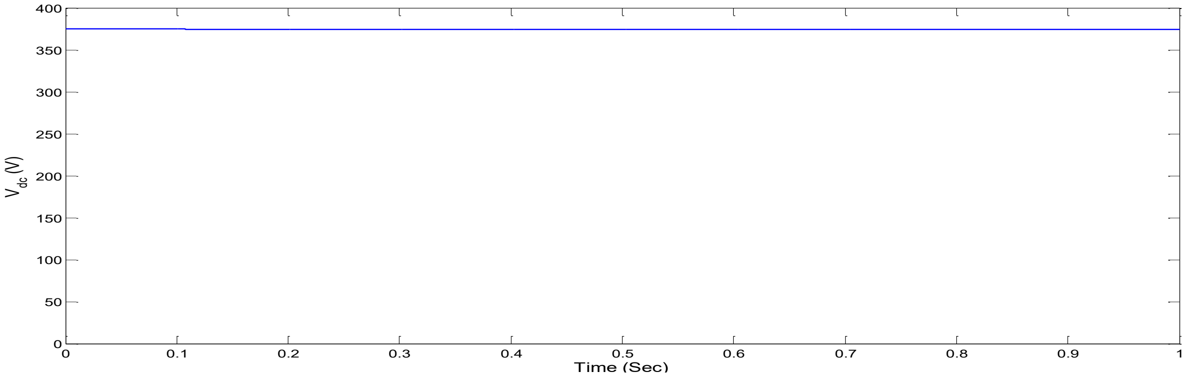

Figure 4 DC link voltage with PR Controller

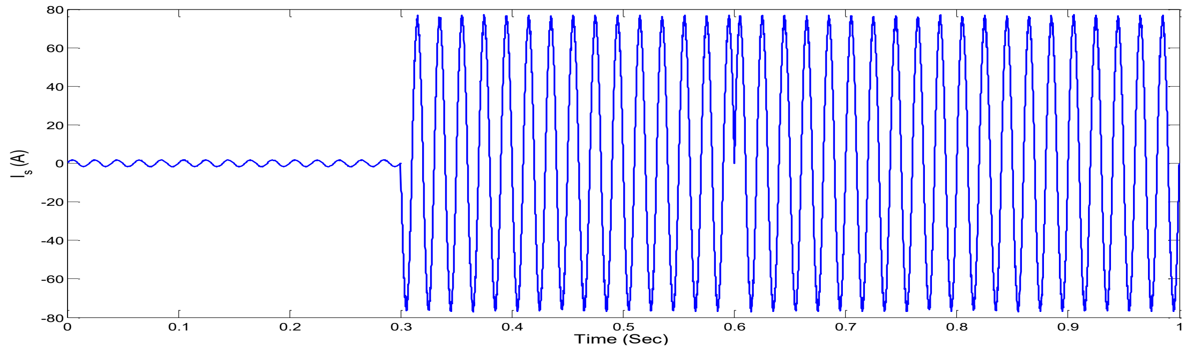

Figure 5 Source current with PR controller

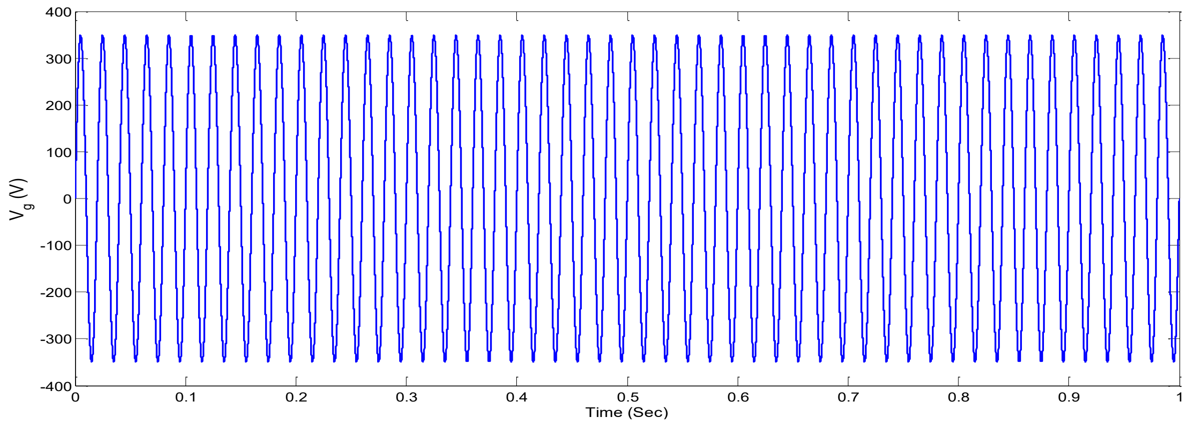

Figure 6 grid voltage with PR controller

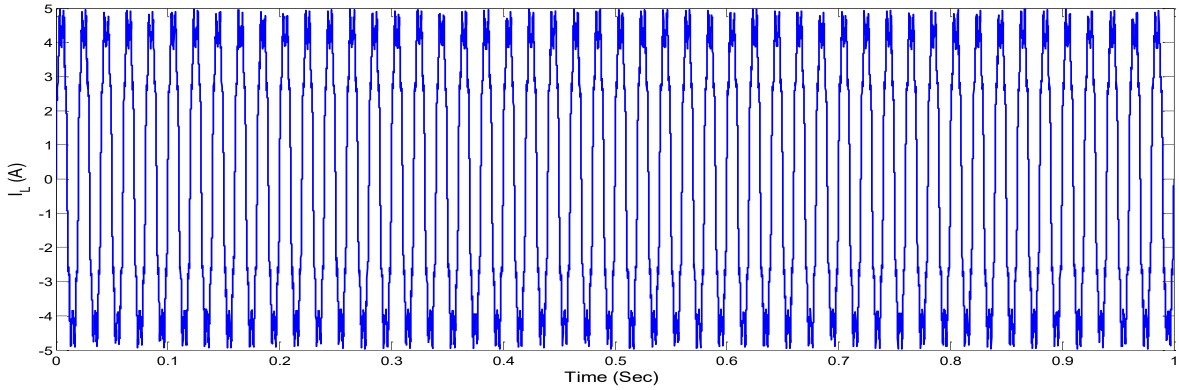

Figure 7 Load current

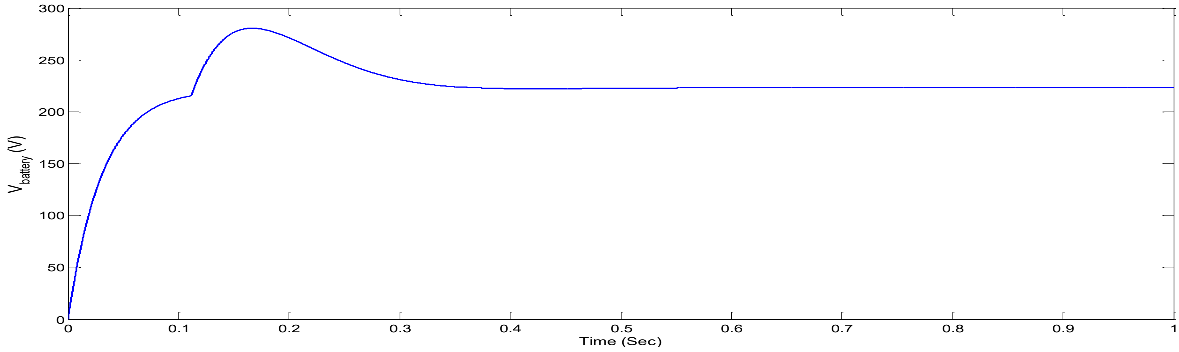

Figure 8 Battery Voltage with proposed controller

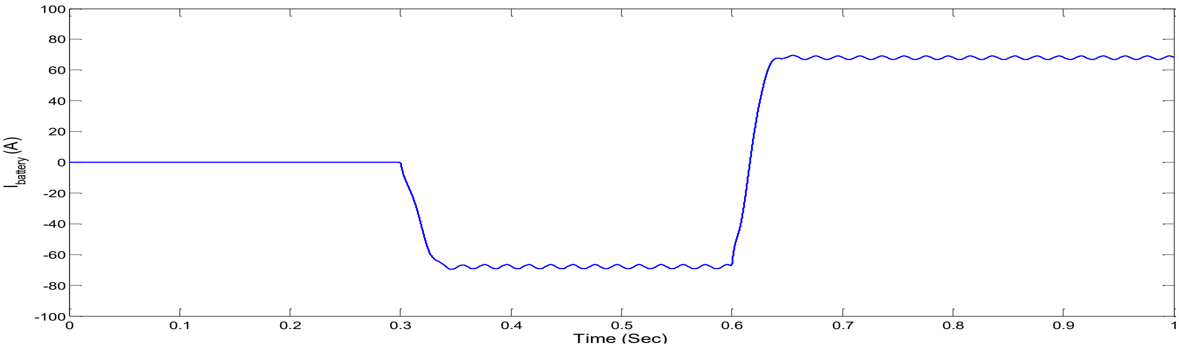

Figure 9 Battery current with proposed controller

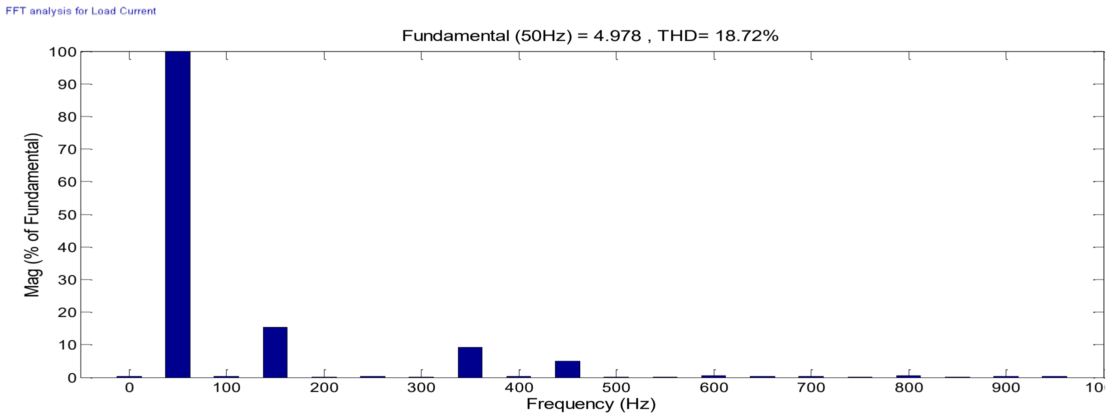

Figure 10 FFT analysis of Load current

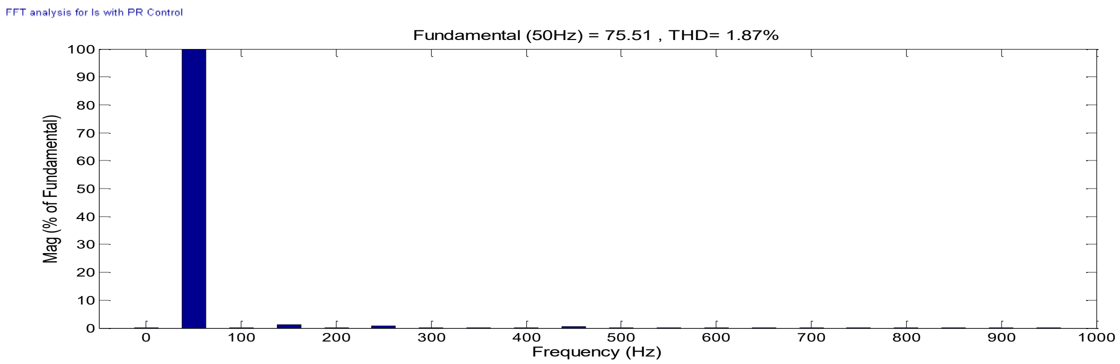

Figure 11 FFT analysis of Source current with PR controller

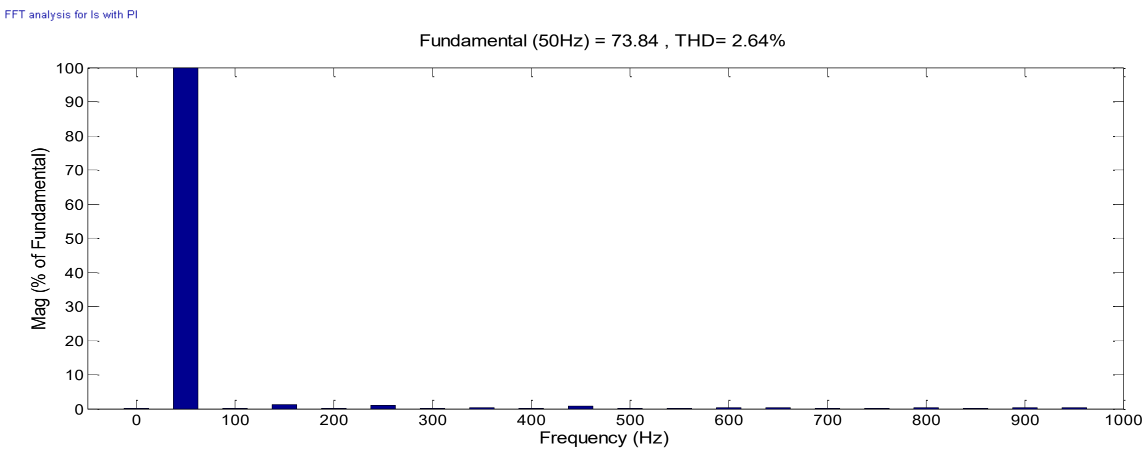

Figure 12 FFT analysis of Source current with PI controller

Under Islanded mode

Effects of increasing sun radiation on the responses shown in Figure 5. Both the grid and the vehicle's battery receive power from the PV array in this case. As electricity is sent into the grid, the voltage and current are not in phase with each other. All the while, the DC link voltage stays the same. A negative battery current flows over the entire electric vehicle battery while charging, raising the voltage to a certain point. The PV voltage (Vpv) is also independent of changes in solar insolation and always equal to the MPPT voltage. With increasing insolation, the PV current grows steadily higher. When solar insolation is higher, more power is available to be fed into the grid. On top of that, the power quality is consistently preserved all the way through.

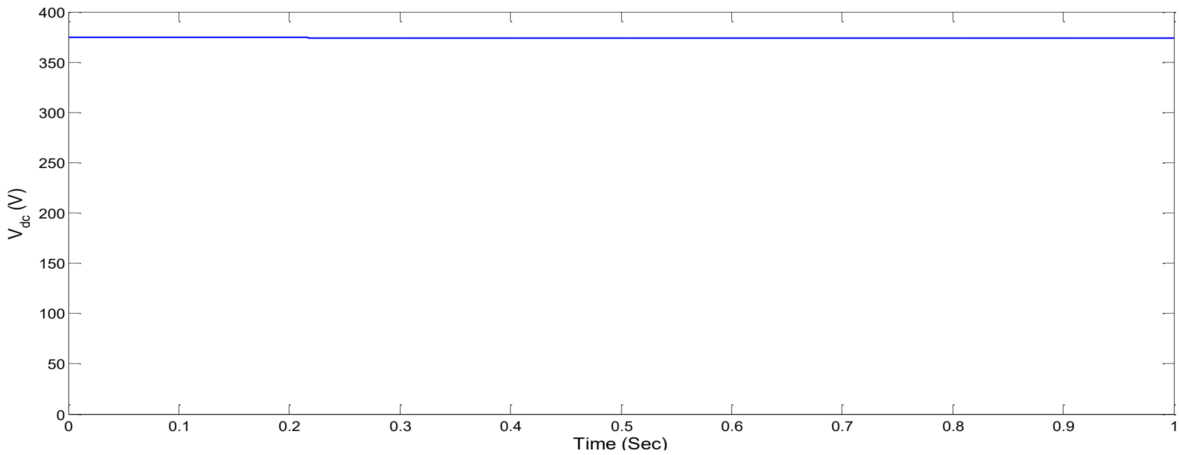

Figure 13 DC link voltage with PR Controller

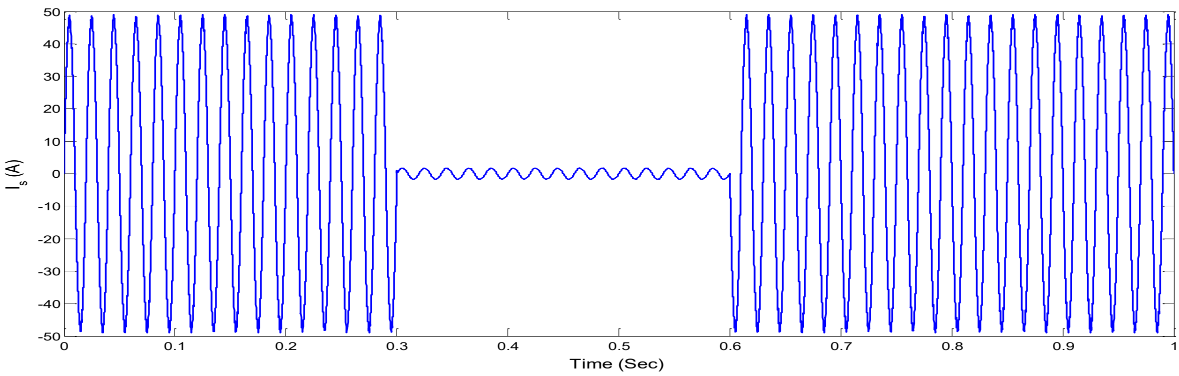

Figure 14 Source current with PR Controller

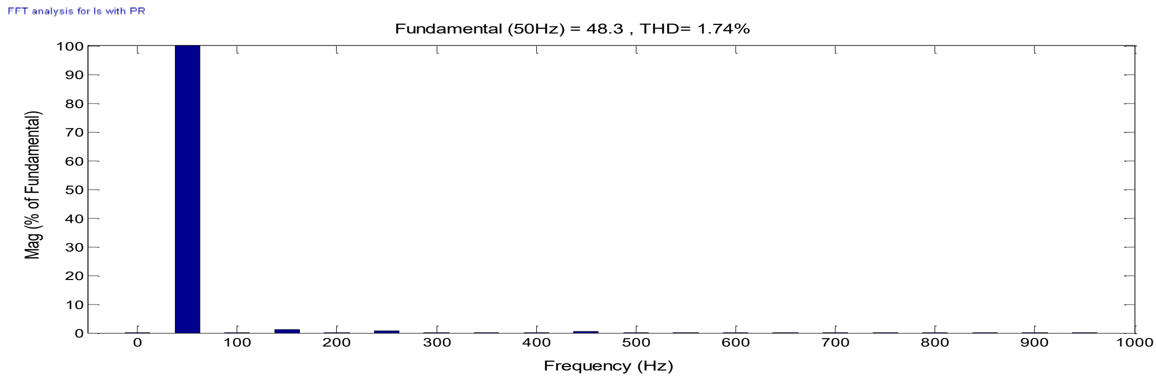

Figure 15 FFT analysis of Source current with PR controller

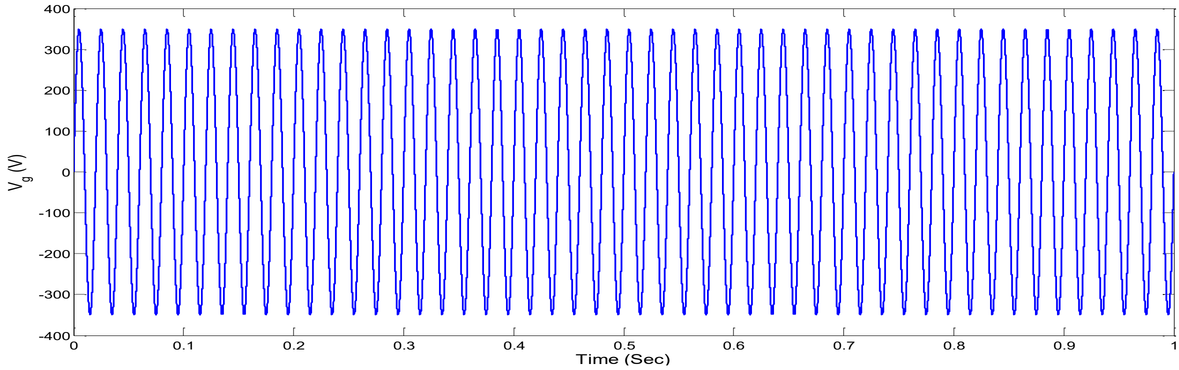

Figure 16 grid voltage with PR controller

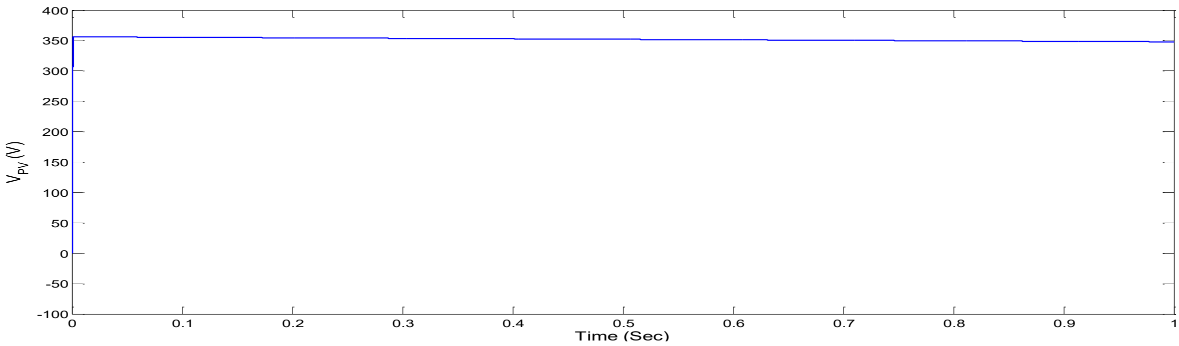

Figure 17 PV output voltage under variation of solar isolation

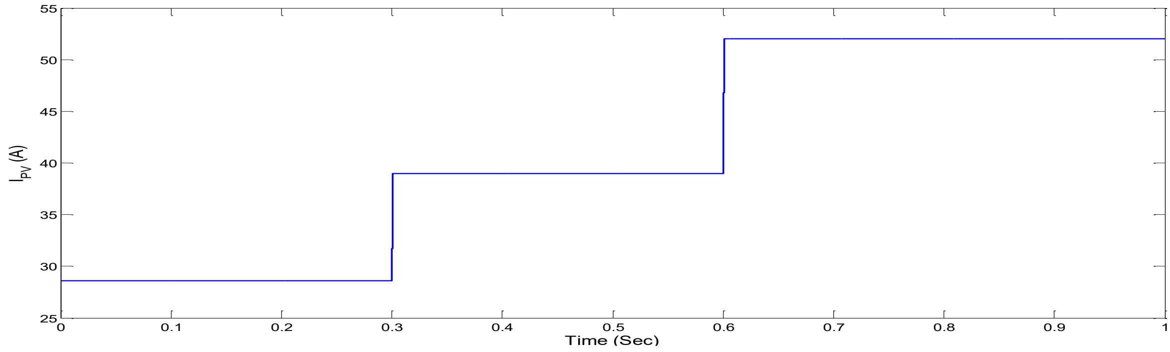

Figure 18 PV output current

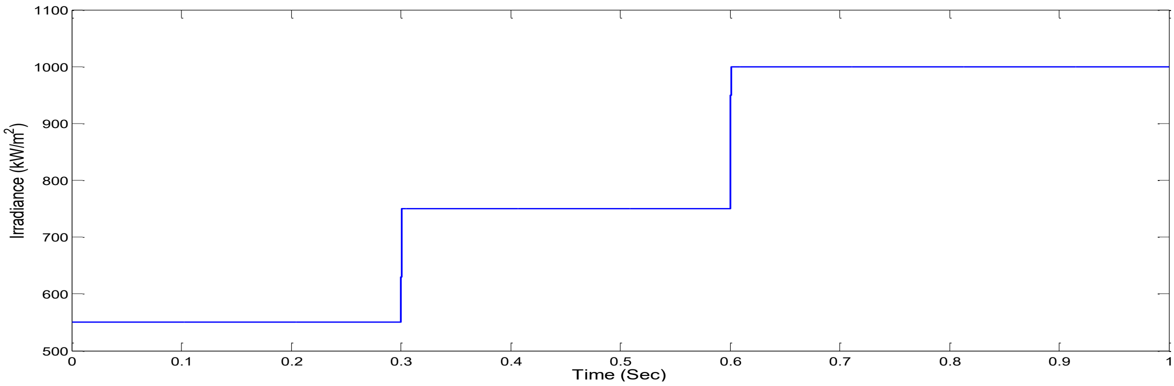

Figure 19 Irradiance input of PV

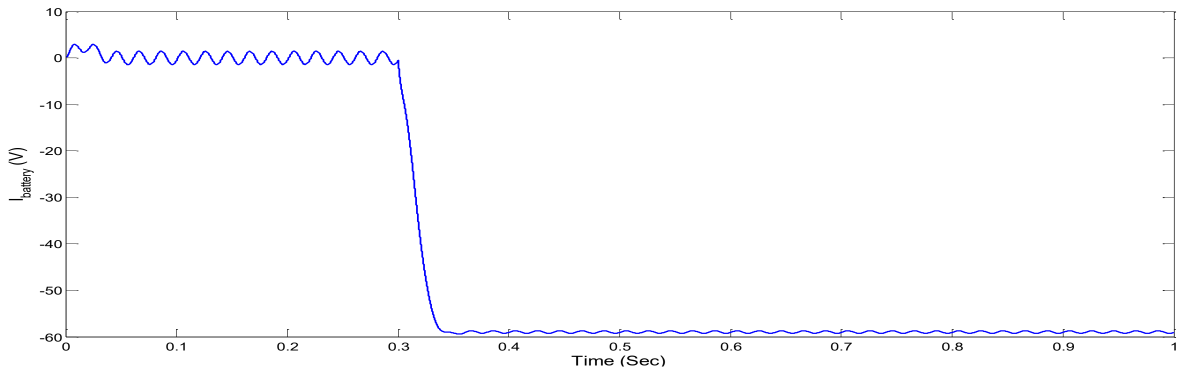

Figure 20 Battery current

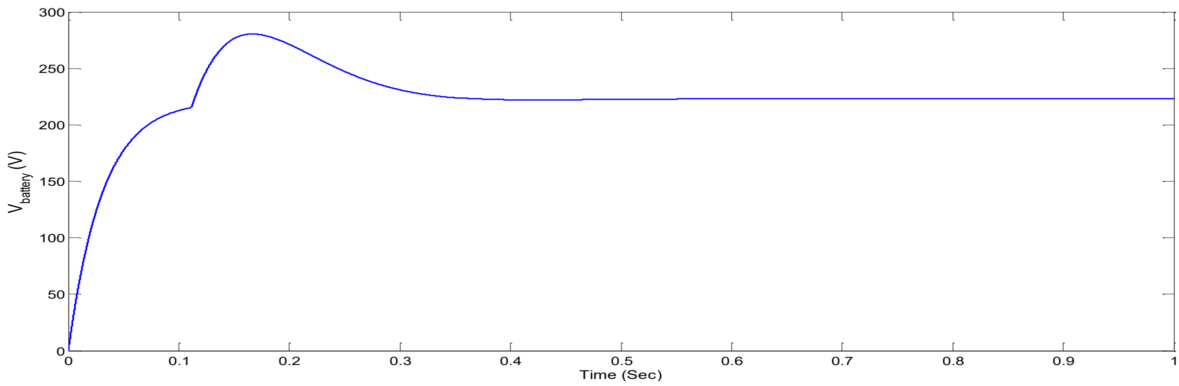

Figure 21 Battery Voltage

IV. Conclusions

The suggested PV-based off-board charging system, which is managed by the JLHCAF algorithm and is connected to the grid via a voltage source converter (VSC), shows strong performance even under changing conditions. System accuracy and stability are greatly improved with the integration of the proportional-resonant (PR) controller. This is especially true when it comes to grid-connected operations, when steady-state errors are eliminated. The PR controller ensures compliance with IEEE power quality requirements by offering greater harmonic compensation and reduced total harmonic distortion (THD) compared to conventional PI control. The system's adaptability is further validated by its bidirectional functionality, capability to manage nonlinear loads, and support for multiple operational modes such as G2V, V2G, PV2G, V2H, and PV2V. An effective solution for current grid-tied electric vehicle (EV) charging applications, the system has been validated by simulations and experimental prototypes to work even under dynamic conditions like load changes and fluctuating solar PV insolation.

References

[1] A Ghazanfari, C Perreault. The path to a vehicle-to-grid future: Powering electric mobility forward. *IEEE Industrial Electronics Magazine*, 2022, 16(3): 4-13.

[2] H Zhao, Y Shen, W Ying, et al. A single- and three-phase grid compatible converter for electric vehicle on-board chargers. *IEEE Transactions on Power Electronics*, 2020, 35(7): 7545-7562.

[3] J Antoun, M Kabir, R Atallah, et al. Assisting residential distribution grids in overcoming large-scale EV
preconditioning load. *IEEE Systems Journal*, 2022, 16(3): 4345-4355.

[4] A Verma, B Singh. AFF-SOGI-DRC control of renewable energy based grid interactive charging station for EV with power quality improvement. *IEEE Transactions on Industry Applications*, 2021, 57(1): 588-597.

[5] I Azeem, M Baig, M Uddin. A strategy to evaluate MPPT techniques. *Asian Conference on Energy*, *Power and Transportation Electrification* (*ACEPT*), 30 October-2 November, 2018, Singapore. IEEE, 2018: 1-4.

[6] J Goud, R Kalpana, B Singh, et al. A global maximum power point tracking technique of partially shaded photovoltaic systems for constant voltage applications. *IEEE Transactions on Sustainable Energy*, 2019, 10(4): 1950-1959.

[7] S S Satapathy, N Kumar. Modulated perturb and observe maximum power point tracking algorithm for solar PV energy conversion system. *3rd International Conference on Recent Developments in Control*, *Automation & Power Engineering*, 10-11 October, 2019, Noida, India. IEEE, 2019: 345-350.

[8] J S Goud, R Kalpna, B Singh, et al. Maximum power point tracking technique using artificial bee colony and hill climbing algorithms during mismatch insolation conditions on PV array. *IET Renewable Power Generation*, 2018, 12: 1915-1922.

[9] G Jagadeesan, R Pitchaimuthu, M Sridharan. A two-stage single-phase grid-connected solar-PV system with simplified power regulation. *Chinese Journal of Electrical Engineering*, 2022, 8(1): 81-92.

[10] A Singh, S Shaha, P G Nikhil, et al. Design and analysis of a solar-powered electric vehicle charging station for Indian cities. *World Electric Vehicle Journal*, 2021, 12(3): 132.

[11] S Arya, R Maurya, J Srikakolapu. Robust iteration-dependent least mean square-based distribution

static compensator using optimized PI gains. *Chinese Journal of Electrical Engineering*, 2022, 8(4): 79-90.

[12] S Kumar, B Singh, A Al-Durra. ℓp-norm proportionate based approach with mode transition between grid interactive and standalone of solar-BES three phase four wire microgrid. *IEEE Transactions on Industry Applications*, 2021, 57(6): 6512-6524.

[13] P Kanjiya, B Singh, A Chandra, et al. “SRF Theory Revisited” to control self-supported dynamic voltage restorer (DVR) for unbalanced and nonlinear loads. *IEEE Transactions on Industry Applications*, 2013, 49(5): 2330-2340.

[14] K Kumar, S S Bhattacharjee, N V George. Joint logarithmic hyperbolic cosine robust sparse adaptive

algorithms. *IEEE Transactions on Circuits and Systems II: Express Briefs*, 2021, 68(1): 526-530.

[15] A Verma, B Singh, A Chandra, et al. An implementation of solar PV array based multifunctional EV charger. *IEEE Transportation Electrification Conference and Expo* (*ITEC*), 2018: 531-536.

[16] B Rajalakshmi, U Soumya, A Kumar. Vehicle to grid bidirectional energy transfer: Grid synchronization using hysteresis current control. *International Conference on Circuit*, *Power and Computing Technologies* (*ICCPCT*), 2017: 1-6.

[17] M Haque, P Wolfs, S Alahakoon, et al. DAB converter with Q capability for BESS/EV applications to allow V2H/V2G services. *IEEE Transactions on Industry Applications*, 2022, 58(1): 468-480.

[18] B Singh, R Kushwaha. Power factor pre regulation in interleaved Luo converter-fed electric vehicle battery charger. *IEEE Transactions on Industry Applications*, 2021, 57(3): 2870-2882.

[19] S M Shariff, M Alam, F Ahmad, et al. System design and realization of a solar-powered electric vehicle charging station. *IEEE Systems Journal*, 2020, 14(2): 2748-2758.

[20] J Gupta, R Maurya, S R Arya. Enhanced performance of on-board EV battery charger with universal power supply. *Electric Power Components and Systems*, 2022, 50(14-15): 840-855.

[21] B Singh, A Verma, A Chandra, et al. Implementation of solar PV-battery and diesel generator based electric vehicle charging station. *IEEE Transactions on Industry Applications*, 2020, 56(4): 4007-4016.

[22] A Verma, B Singh. Multimode operation of solar PV array, grid, battery and diesel generator set based EV charging station. *IEEE Transactions on Industry Applications*, 2020, 56(5): 5330-5339.

[23] D Mishra, B Singh, B K Panigrahi. Sigma-modified power control and parametric adaptation in a grid-integrated PV for EV charging architecture. *IEEE Transactions on Energy Conversion*, 2022, 37(3): 1965-1976.

[24] V Jain, B Singh, Seema. A grid connected PV array and battery energy storage interfaced EV charging station. *IEEE Transactions on Transportation Electrification*, 2023, 9(3): 3723-3730.

[25] S Pranith, S Kumar, B Singh, et al. Improved Gaussian filter based solar PV-BES microgrid with PLL based islanding detection and seamless transfer control. *IEEE Transactions on Industrial Electronics Electronics*, 2022, 69(6): 5815-5825.

[26] D Jaraniya, S Kumar. PV charging station with VSS-IMSAF and SOSMCC disturbance observer based

controls to enhance the distribution grid capability. *IETE Journal of Research*, 2023-01-01. DOI: https://doi.org/10.1080/ 03772063.2023.2169201.

[27] N Kumar, S Panda. A multipurpose and power quality improved electric vesels charging station for the seaports. *IEEE Transactions on Industrial Informatics*, 2023, 19(3): 3254-3261.